0026-895X/92/020281-09$03.00/0

MOLECULAR PHARMACOLOGY, 41:281-289

Platelet-Activating Factor Stimulates Phosphoinositide Turnover in Neurohybrid NCB-20 Cells: Involvement of Pertussis Toxin-Sensitive Guanine Nucleotide-Binding Proteins and Inhibition by Protein Kinase C

TIAN-LI YUE, JEFFREY M. STADEL, HENRY M. SARAU, EITAN FRIEDMAN, JUAN-LI GU, DAVID A. POWERS, MARIE M. GLEASON, GIORA FEUERSTEIN, and HOAU-YAN WANG

Department of Pharmacology, SmithKline Beecham Pharmaceuticals, King of Prussia, Pennsylvania 19406 (T.-L.Y., J.M.S., H.M.S., J.-L.G., D.A.P., M.M.G., G.F.), and Division of Neurochemistry, Medical College of Pennsylvania, Philadelphia, Pennsylvania 19129 (E.F., H.-Y.W.)

Received March 21, 1991; Accepted October 24, 1991

SUMMARY

Platelet-activating factor (PAF) is an unusually potent phospholipid known to be produced by neuronal cells and to modulate cerebral blood flow and metabolism. In previous studies with NCB-20 cells, we reported that PAF induced a significant mobilization of intracellular free Ca^{2+} ($[Ca^{2+}]_i$), which was inhibited by PAF antagonists. The increase was the result of release from intracellular stores and influx from extracellular sources. The present study was designed to characterize further PAF receptor-mediated cellular signal-transduction mechanisms in *myo*-[^{3}H]inositol-labeled cells. PAF induced a concentration-dependent increase in phosphatidylinositol (PI) metabolism, with EC_{50} values of 1.96 ± 0.62 nM and 1.12 ± 0.50 nM for inositol trisphosphate (IP_3) and inositol monophosphate (IP_1) formation, respectively (four experiments). The maximal production of IP_3 and IP_1 induced by 50 nM PAF was 254 ± 34% and 178 ± 25% over the basal, respectively (four experiments). PAF-induced PI metabolism was concentration-dependently inhibited by the PAF antagonist BN50739, with an IC_{50} value of 6.48 ± 0.52 nM (four experiments). The protein kinase C (PKC) activator phorbol 12,13-dibutyrate concentration-dependently inhibited PAF-induced PI metabolism and $[Ca^{2+}]_i$ mobilization in NCB-20 cells, which was partially prevented by the PKC inhibitor H-7. Pretreatment of NCB-20 cells with pertussis toxin (PTX) resulted in a concentration-dependent inhibition of PAF-induced IP_3 production and intracellular Ca^{2+} release, with a maximal reduction of 66.9 ± 3.5% and 63 ± 6.1%, respectively, at 300 ng/ml PTX. PTX in the presence of [^{32}P]NAD specifically [^{32}P]ADP-ribosylated a 38-kDa protein in membranes prepared from NCB-20 cells. Pretreatment of the cells with PTX resulted in a concentration-dependent inhibition of subsequent ^{32}P-labeling of the toxin substrate in the membranes and correlated with the uncoupling of PAF-induced IP_3 formation. PAF (0.01–10 nM) elicited a concentration-related stimulation in guanosine 5′-*O*-(3-[^{35}S]) triphosphate ([^{35}S]GTPγS) binding to $G_{\alpha i(1,2)}$ proteins, which was inhibited by the PAF antagonist BN50739. PAF at 10 nM also increased [^{35}S]GTPγS binding to $G_{\alpha s}$ and $G_{\alpha o}$. PAF-evoked activation of $G_{\alpha i(1,2)}$ and $G_{\alpha o}$ was reduced by preincubation with PTX. Our results reveal that neuronal cells possess PAF receptors linked through guanine nucleotide-binding proteins to phospholipase C and receptor-operated Ca^{2+} channels that are regulated by PKC. Both PTX-sensitive and -insensitive guanine nucleotide-binding proteins appear to couple the PAF receptor to activation of phospholipase C and the increase in $[Ca^{2+}]_i$. These results contribute to the further understanding of the mechanisms behind PAF actions on neuronal cells.

PAF (1-*O*-alkyl-2 acetyl-*sn*-glycero-3-phosphocholine) is a lipid autacoid with many diverse potent physiological effects. It is now clear that PAF can be produced by many different cell types and is involved in a variety of pathological responses, such as allergic and inflammatory reactions, endotoxic shock, and ischemia-induced tissue damage (1, 2).

PAF exerts its effects via a cellular receptor, which has recently been cloned and sequenced (3). An increasing body of evidence suggests that biological responses of PAF occur via receptor-mediated signal transduction mechanisms (4). Although most PAF studies have been conducted in platelets, some controversial results have been found in other cell types. For example, the G protein coupled to the PAF receptor in human platelets is different from that in human neutrophils (5).

PAF has been found in the CNS (6–8), and its production by

ABBREVIATIONS: PAF, platelet-activating factor; PI, phosphatidylinositol; IP_1, inositol monophosphate; IP_2, inositol bisphosphate; IP_3, inositol trisphosphate; IP_4, inositol tetrakisphosphate; PTX, pertussis toxin; PKC, protein kinase C; PDBu, phorbol 12,13-dibutyrate; $[Ca^{2+}]_i$, cytosolic free calcium concentration; G protein, guanine nucleotide-binding regulatory protein; CNS, central nervous system; GTPγS, guanosine 5′-*O*-(3-thio)triphosphate; KRH, Krebs-Ringer Henseleit; EGTA, ethylene glycol bis(β-aminoethyl ether)-*N,N,N′,N′*-tetraacetic acid; HPLC, high performance liquid chromatography; 4α-PDD, 4α-phorbol 12,13-didecanoate; PLC, phospholipase C; TCA, trichloroacetic acid; SDS, sodium dodecyl sulfate; DMEM, Dulbecco's modified Eagle's medium; KRB, Krebs-Ringer buffer; HEPES, 4-(2-hydroxyethyl)-1-piperazineethane-sulfonic acid.

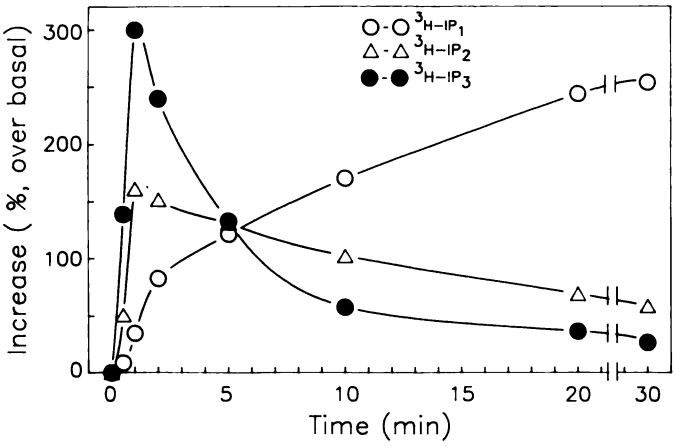

Fig. 1. Time course of PAF-induced formation of [^{3}H]IP$_1$, [^{3}H]IP$_2$, and [^{3}H]IP$_3$ in NCB-20 cells. NCB-20 cells were prelabeled with *myo*-[^{3}H] inositol, in inositol-free DMEM, overnight and were washed twice with KRH buffer. The cells were preincubated at 37° for 30 min in the presence of 10 mM $LiCl_2$ before addition of 50 nM PAF or saline. The reaction was stopped at the indicated times, and [^{3}H]inositol phosphates were separated by anion exchange resin open column chromatography. The basal values of [^{3}H]IP$_1$, [^{3}H]IP$_2$, and [^{3}H]IP$_3$ were 9651 ± 428, 2572 ± 54, and 549 ± 55 dpm, respectively, and did not change significantly during 30 min of incubation. Each *point* is the mean of triplicate determinations from a representive experiment, which was repeated three times with similar results.

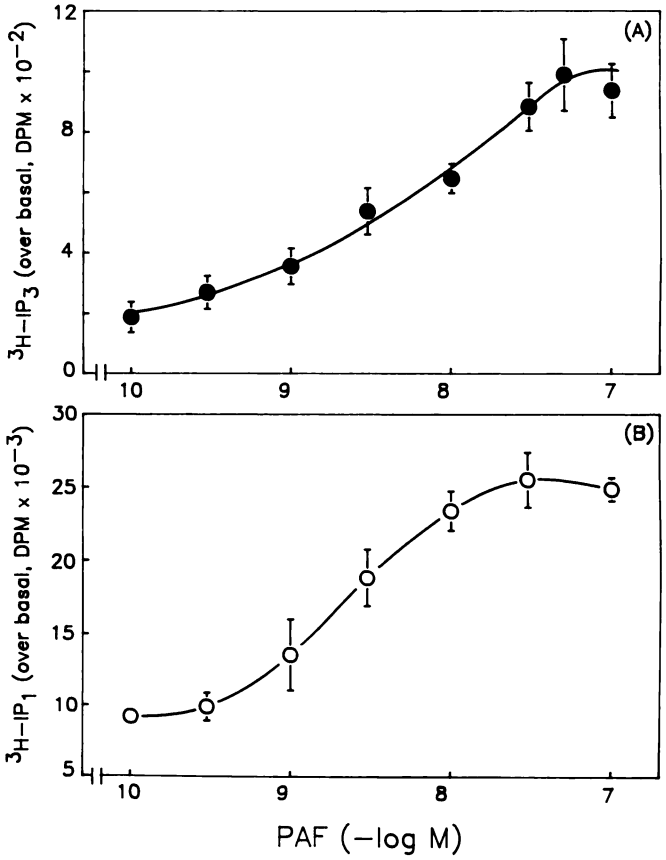

Fig. 2. Concentration dependence of PAF-stimulated production of [^{3}H] IP$_1$ (B) and [^{3}H]IP$_3$ (A) in NCB-20 cells. The experimental conditions are as described in the legend to Fig. 1. The stimulation was terminated at 1 min (for [^{3}H]IP$_3$) or 30 min (for [^{3}H]IP$_1$) after addition of PAF. Results are expressed as means ± standard errors of four independent experiments performed in triplicate. The basal values of [^{3}H]IP$_1$ and [^{3}H]IP$_3$ were 8447 ± 566 and 433 ± 53 dpm, respectively.

neuronal cells has been confirmed recently in our laboratory (9) and others (10). Specific binding sites for PAF have been found in synaptosomes and microsomal fractions of rat cerebral cortex (11), as well as gerbil brain tissue (12). A role for PAF as a putative mediator in CNS injury, particularly in brain ischemia and traumatic injury-induced neuronal damage, has been suggested, because the levels of PAF are significantly increased and the PAF antagonists have protective effects in these CNS pathological states (for review, see Ref. 13).

The effects of PAF on cerebral circulation and brain function have been observed *in vivo* and *in vitro* (14, 15). However, little information is available regarding functional studies of PAF at the cellular level of neuronal tissue, particularly with respect to signal-transduction mechanisms. In a previous study (16), we reported that PAF induced a significant transient increase in $[Ca^{2+}]_i$ in NCB-20 cells, a hybrid of mouse neuroblastoma and Chinese hamster embryonic brain cells. A portion of the PAF-induced elevation of $[Ca^{2+}]_i$ in NCB-20 cells was contributed by release of intracellular calcium, suggesting the possible involvement of PI metabolites induced by PAF. Therefore, the present study was undertaken to examine the effects of PAF on PI metabolism and to elucidate further the mechanisms involved in regulation of PAF receptor-mediated signal transduction in NCB-20 cells.

Materials and Methods

Chemicals. Synthetic PAF (1-*O*-hexadecyl-2-acetyl-*sn*-glyceryl-3-phosphorylcholine) was kindly provided as a gift from Dr. F. Snyder (Oak Ridge Associated University, Oak Ridge, TN). PAF was dissolved in $CHCl_3$-/methanol (9:1), to a concentration of 10 nmol/ml, and was stored at −70° as a stock solution. Before use, the solution was evaporated under nitrogen and redissolved in saline containing 0.25% bovine serum albumin. BN 50739 [tetrahydro-4,7,8,10-methyl-(chloro-2-phenyl)-6-[(dimethoxy-3,4-phenyl)thio]methylthiocarbonyl-9-pyrido[4′,3′,4,5]thieno[3,2-*f*]triazolo-1,2,4[4,3-*a*]diazepine-1,4] was kindly provided by Dr. P. Braquet (Institute Henri Beaufour, Paris, France). BN 50739 was first solubilized in a small volume of dimethylsulfoxide and diluted with saline as described previously (17). The final concentration of dimethylsulfoxide was <0.1%. Fura-2/pentaacetoxymethyl ester and AG 1-X8 anion exchange resin (200–400 mesh) were obtained from Calbiochem (La Jolla, CA) and Bio-Rad (Richmond, CA), respectively. *myo*-[^{3}H]Inositol (specific activity, 17.4 Ci/mmol) was purchased from Amersham. PTX was obtained from List Biological Laboratories (Campbell, CA). H-7 [1-(5-isoquinolinylsulfonyl)-2-methylpiperazine dihydrochloride] was purchased from Research Biochemicals, Inc. (Natick, MA). [^{35}S]GTPγS (1311 Ci/mmol), G protein antipeptide antibodies, and [^{32}P]NAD (30 Ci/mmol) were purchased from NEN (Boston, MA). NCB-20 cells were kindly provided by Dr. M. Nirenberg (National Heart, Lung, and Blood Institute, National Institutes of Health). All other reagents were obtained from Sigma Chemical Co. (St. Louis, MO).

Cell culture. NCB-20 cells were grown in DMEM supplemented with 10% (v/v) heat-inactivated fetal calf serum, 0.1 mM hypoxanthine, 0.4 μM aminopterin, and 16 μM thymidine, in a humidified environment of 5% CO_2/95% air at 37°. They were initially cultured in 150-cm^2 flasks. After reaching confluence, NCB-20 cells were harvested by treatment with 0.05% trypsin/0.53 mM EDTA and were then subcultured into six-well (35-mm) dishes for the study of PI metabolism. Cells from passages 5–20 were used in this study.

Separation and measurement of inositol phosphates by anion exchange open column chromatography. NCB-20 cells were grown to approximately 90% confluence and prelabeled with *myo*-[^{3}H]inositol (2 μCi/ml) (in 35-mm Petri dishes), in inositol-free DMEM containing 10% (v/v) dialyzed fetal calf serum, overnight. The cells were washed

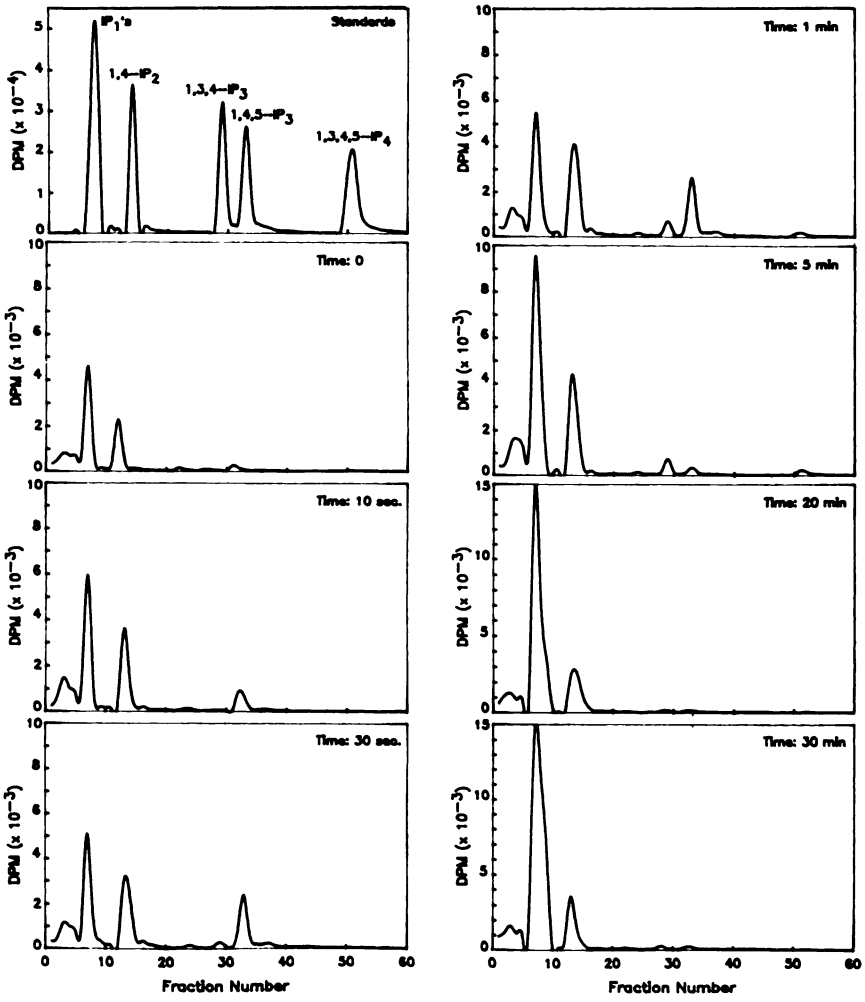

Fig. 3. HPLC separation of inositol phosphates induced by 50 nM PAF in NCB-20 cells, at different times as indicated. The samples were prepared and fractionated by HPLC, using an anion exchange column (Beckman Ultrasil 10-SAX column, 25 × 0.46 cm), as described in Materials and Methods. The flow rate was 1.25 ml/min, and 0.3-ml fractions were collected and counted. Each sample was from pooling of the cells from six 35-mm wells.

TABLE 1

Effect of BN 50739 on PAF-induced IP_3 formation in NCB-20 cells

myo-[^{3}H]Inositol-labeled NCB-20 cells were pretreated with BN 50739 for 1 min at 37°, and then 50 nM PAF was added. The reaction was stopped by addition of 100 μl of 100% TCA 1 min after PAF stimulation. [^{3}H]IP_3 was separated by anion exchange chromatography and the radioactivity was counted as described in Materials and Methods. Each value represents the mean ± standard error of four different experiments done in triplicate.

BN 50739	[^{3}H]IP_3 formation (over basal)	Inhibition
nM	*dpm*	%
0	915 ± 44	
1	784 ± 42	14.3
3	586 ± 61	36.0
10	362 ± 90	60.4
30	229 ± 82	75.1
60	56 ± 8	93.9

twice with KRH buffer containing 0.1% bovine serum albumin, 118 mM NaCl, 4.6 mM KCl, 24.9 mM $NaHCO_3$, 1.0 mM KH_2PO_4, 11.1 mM glucose, 1.1 mM $MgSO_4$, 5.0 mM HEPES, and 1.0 mM $CaCl_2$, pH 7.4, and then 1 ml of KRH buffer containing 10 mM LiCl was added to each well. The cells were preincubated for 30 min at 37°, and the reaction was initiated by the addition of PAF and continued for various times as indicated in the figures. The reaction was terminated by addition of 100 μl of 100% TCA. Samples were maintained on ice for 20 min and the cells were scraped and transfered with the supernatant to a 1.5-ml Eppendorf tube. After centrifugation, the supernatant (0.9 ml/sample) was removed to a 10-ml glass tube. TCA was extracted from the supernatant with 6 × 2 ml of water-saturated diethylether. Excess ether was evaporated under nitrogen, and the samples were neutralized with 10 μl of 0.5 M Tris base (final pH, 7–7.2). Samples were stored frozen (−80°) until the inositol phosphates were separated by open column chromatography or HPLC.

Samples prepared as described above were mixed with 2 ml of 5 mM sodium tetraborate containing 0.5 mM EDTA and were poured onto disposable polystyrene columns (1 × 10 cm) containing 0.5 g of AG 1 × 8 anion exchange resin (formate form). *myo*-[^{3}H]Inositol was eluted with 5 ml of 20 mM ammonium formate. [^{3}H]IP_1, [^{3}H]IP_2, and [^{3}H]IP_3 were sequentially eluted into scintillation vials with 4 ml of 0.2, 0.4, and 0.8 M ammonium formate, respectively, containing 0.1 M formic acid. Ten milliliters of scintillation solution (Ready Gel; Beckman) were added to the vials, and the radioactivity was determined with a counting efficiency of approximately 30%.

Separation of IP_3 isomers by HPLC. The samples prepared as described above were lyophilized to dryness, reconstituted with 1.2 ml of H_2O, and filtered through Millipore HV filters (0.45 μm). Samples (1.0 ml) were injected and fractionated on an anion exchange column (Beckman Ultrasil 10-SAX column, 25 × 0.46 cm) with a discontinuous gradient from 0 to 3.5 M ammonium formate (pH 3.7 with phosphoric acid), as described by Hawkins *et al.* (18). The flow rate was 1.25 ml/min, 0.3-ml fractions were collected, 4 ml of Tru-Count (IN/US) were added to each fraction, and the radioactivity was quantitated.

Measurement of $[Ca^{2+}]_i$ mobilization. $[Ca^{2+}]_i$ was measured as described previously (19). Briefly, the harvested cells were resuspended at 2 × 10^6/ml in KRH buffer and were incubated with 2 μM fura-2/acetoxymethyl ester at 37° for 45 min. The cells were centrifuged, resuspended in KRH buffer, and incubated at 37° for an additional 20 min, to allow for complete hydrolysis of entrapped ester. Cells were

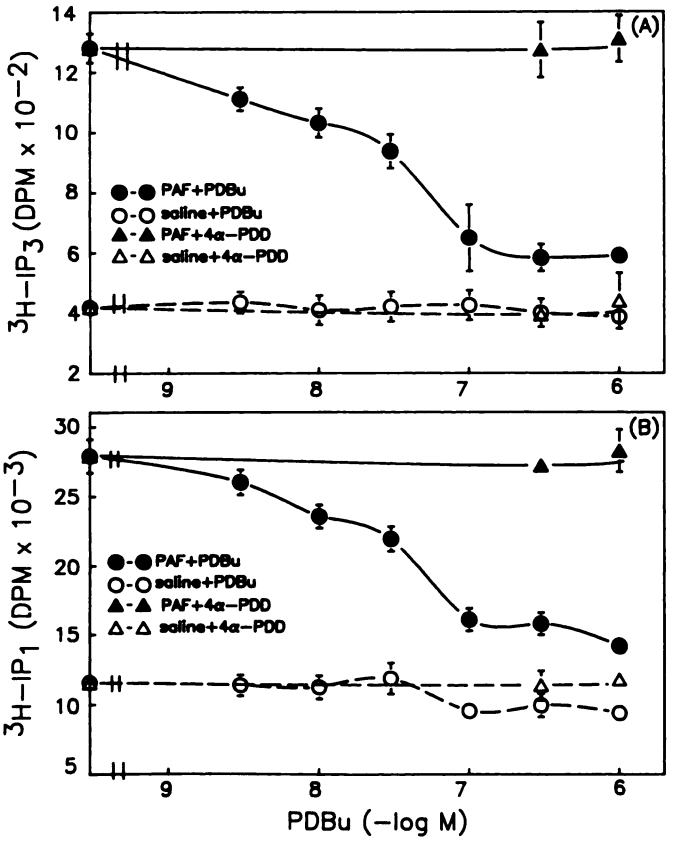

Fig. 4. Effects of phorbol ester on PAF-induced production of [^{3}H]IP$_3$ (A) and [^{3}H]IP$_1$ (B) in NCB-20 cells. Experimental conditions are as described in the legend to Fig. 1, except that indicated concentrations of PDBu or 4α-PDD were added 10 min before the addition of 50 nM PAF or vehicle (basal). The reaction was stopped at 1 min (for IP$_3$) or 30 min (for IP$_1$) after addition of PAF. Data presented are means ± standard errors of three independent experiments done in triplicate. PAF (50 nM)-induced production of IP$_3$ at 1 min and IP$_1$ at 30 min was 230% and 141%, respectively, over the basal level in the absence of PDBu.

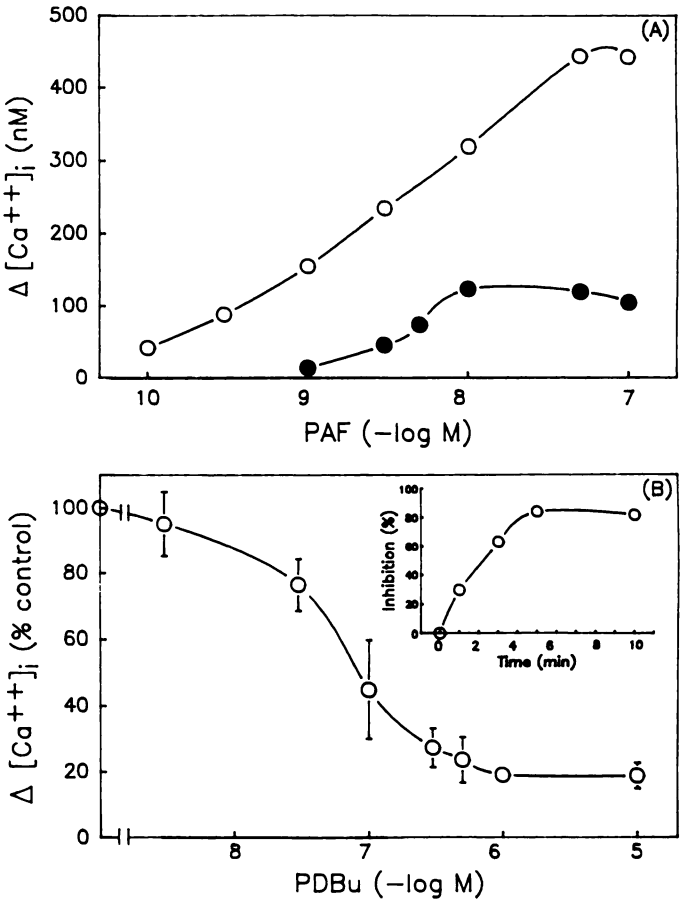

Fig. 5. Effects of phorbol ester on PAF-induced elevation of [Ca^{2+}]$_i$ in NCB-20 cells. A, Shift of PAF dose-response curve (○, Control) in the presence of 300 nM PDBu (●). The cells were preincubated with PDBu at 37° for 5 min and then challenged with PAF at the concentrations indicated. Δ [Ca^{2+}]$_i$ is the value obtained by subtracting basal preagonist value from the peak postagonist value. Each *point* represents the mean of duplicate samples. B, Inhibition of 50 nM PAF-induced [Ca^{2+}]$_i$ increase in NCB-20 cells by various concentrations of PDBu. Cells were preincubated with PDBu at 37° for 5 min and then challenged with PAF (50 nM). The maximal increase in [Ca^{2+}]$_i$ induced by PAF in the absence of PDBu was 398 ± 32 nM and was assumed to be 100% of control. *Inset*, time course of PDBu (300 nM) to inhibit 50 nM PAF-induced [Ca^{2+}]$_i$ elevation.

washed and resuspended in KRH buffer at 10^6 cells/ml. The fluorescence of fura-2-containing cells was measured with a spectrofluorometer designed by the Biomedical Instruments Group, University of Pennsylvania. The wavelengths were set at 339 nm for excitation and 505 nm for emission. All experiments were performed at 37°. For the studies in Ca^{2+}-free KRH, fura-2-loaded cells were centrifuged, resuspended in prewarmed (37°) Ca^{2+}-free KRH buffer containing 1.0 mM EGTA, and used immediately.

[^{35}S]GTPγS binding to G proteins and immunoprecipitation. NCB-20 cells were washed twice in 10 ml of ice-cold phosphate-buffered saline, pH 7.2, containing 1.8 mM KH_2PO_4, 137 mM NaCl, 2.7 mM KCl, and 10 mM Na_2HPO_4, and were centrifuged at 3000 × *g* for 10 min at 4°. The cells were resuspended in 10 volumes of oxygenated KRB, pH 7.4, containing 1.2 mM KH_2PO_4, 118 mM NaCl, 4.8 mM KCl, 1.3 mM $CaCl_2$, 1.2 mM $MgSO_4$, 25 mM $NaHCO_3$, 10 mM glucose, and 0.1 mM ascorbic acid, homogenized in a glass/Teflon homogenizer, and then sonicated for 5 sec. The homogenate was centrifuged at 48,000 × *g* for 10 min, and the pellet was resuspended in 10 volumes of KRB. Protein values were determined by the method of Lowry *et al.* (20), and 100 μg of membrane protein were used to assay for [^{35}S]GTPγS binding. Membrane proteins were preincubated with 2 nM [^{35}S]GTPγS (1311 Ci/mmol) for 5 min at 25°, followed by the addition of PAF. Incubation continued for 5 min. To examine the effects of the antagonist, BN 50739 was added 5 min before the addition of [^{35}S]GTPγS. To assess the effectiveness of toxins, tissues were incubated with PTX or cholera toxin for 2 hr before the incubation with [^{35}S]GTPγS. The reactions were terminated by the addition of 250 μl of ice-cold KRB containing 50 mM EDTA and were centrifuged at 12,000 × *g* for 5 min. The membranes were solubilized in 500 μl of immunoprecipitation buffer containing 100 mM Tris, pH 7.4, 2.5% (v/v) Nonidet P-40, 200 mM NaCl, and 10 mM EDTA, with 0.2% SDS, by sonication for 10 sec, followed by the addition of 500 μl of buffer. Immunoprecipitation was carried out using a modification of the method described by Romano *et al.* (21). The suspensions were precleared by the addition of 10 μl of normal rabbit serum (1/100 dilution; Calbiochem) and incubation at 25°. After 30 min, 100 μl of a 10% suspension of Protein A-bearing *Staphylococcus aureus* cells (Pansorbin cells; Calbiochem) were added and incubated for 30 min. The suspension was centrifuged, and $G_{\alpha i(1,2)}$, $G_{\alpha s}$, or $G_{\alpha o}$ antipeptide antiserum (1/1000 dilution) or normal rabbit serum (1/1000) was added to the supernatant and incubated for 30 min at 25°. Pansorbin cells (100 μl) were added and incubated for 30 min. The Protein A-antibody-antigen complex was collected by centrifugation and washed with precipitation buffer. The resulting pellet was resuspended in KRB by brief sonication, and radioactivity was measured by liquid scintillation counting. The radioactivity precipitated by normal rabbit serum was considered background and was subtracted from all values. Agonist-induced stimulation of [^{35}S]GTPγS binding to G proteins was calculated as percentage above unstimulated control values.

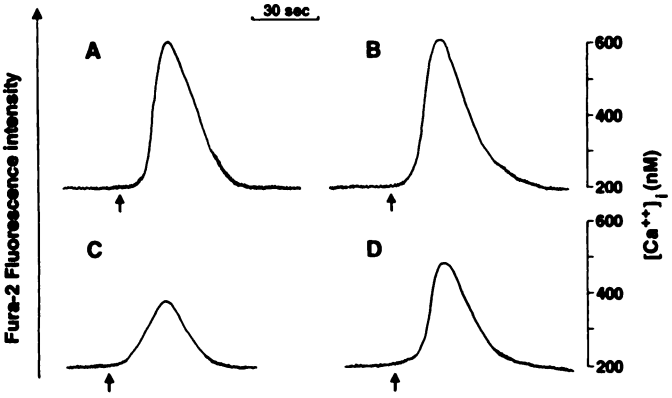

Fig. 6. H-7 blocks the PDBu inhibition of PAF-induced $[Ca^{2+}]_i$ elevation in fura-2-loaded NCB-20 cells. *Trace A*, 50 nM PAF alone (control); *trace B*, cells treated with 100 μM H-7 at 37° for 10 min and then stimulated with 50 nM PAF; *trace C*, cells treated with 100 nM PDBu at 37° for 5 min and then stimulated with 50 nM PAF; *trace D*, cells treated with 100 μM H-7 for 5 min and then with 100 nM PDBu for another 5 min before stimulation with 50 nM PAF. *Arrow*, time at which PAF was added. *Right vertical scale*, result of transforming fluorescent output to $[Ca^{2+}]_i$ (nM).

TABLE 2

Effect of H-7 on inhibition of PAF-induced IP_3 production by PDBu

myo-[^{3}H]Inositol-labeled NCB-20 cells were preincubated with H-7 or vehicle for 5 min at 37°, and then PDBu was added and incubation was continued for 5 min before addition of 50 nM PAF. The reaction was stopped by addition of 100 μl of 100% TCA 1 min after PAF stimulation. [^{3}H]IP_3 was separated by open column anion exchange chromatography, and the radioactivity was counted as described in Materials and Methods. Each value represents the mean ± standard error of three different experiments done in triplicate.

Treatment	[^{3}H]IP_3 formation (over basal)	Inhibition
	dpm	%
PAF	750 ± 18	
PDBu (30 nM) + PAF	568 ± 25	24.3
H-7 (10 μM) + PDBu (30 nM) + PAF	659 ± 49	12.1
PDBu (100 nM) + PAF	358 ± 48	53.3
H-7 (100 μM) + PDBu (100 nM) + PAF	479 ± 57	36.1

ADP-ribosylation. Cell membrane labeling with [^{32}P]NAD was a modification of procedures described previously (22). Briefly, the cell lysates were homogenized by 10 strokes in a Dounce homogenizer and then centrifuged at 1000 × *g* for 10 min. The supernatants were harvested and centrifuged at 40,000 × *g* for 15 min. The resulting membrane pellets were resuspended in buffer containing 12.5 mM $MgCl_2$, 1.5 mM EDTA, 0.5 mM dithiothreitol, and 75 mM Tris (pH 7.5), and the protein concentrations were adjusted to 2 mg/ml. The membrane suspensions (0.1 ml) were incubated for 30 min at 37° with 20 mM thymidine, 1 mM ATP, 0.5 mM GTP, 75 μM $NADP^+$, 0.1 mM nicotinamide, 5 μM [^{32}P]NAD, and 5 μg/ml PTX (pretreated with 20 mM dithiothreitol for 10 min at 37°). At the end of the 30-min incubation, the membranes were washed and solubilized in SDS sample buffer, and SDS-polyacrylamide gel electrophoresis was carried out (22). Autoradiograms were analyzed using the Hewlett-Packard DeskScan Image Analyzer, and the data were quantified using Fotodyne's College Analysis Software.

Statistics. Data in the text and figures are mean ± standard error for the indicated number (*n*) of experiments. The Student's *t* test was used for statistical analysis. Significant differences were accepted at $p < 0.05$.

Results

PAF-induced phosphoinositide turnover in NCB-20 cells. Addition of PAF to cultured NCB-20 cells prelabeled with *myo*-[^{3}H]inositol in the presence of lithium resulted in a substantial increase in the production of [^{3}H]IP_1, [^{3}H]IP_2, and [^{3}H]IP_3. Rapid [^{3}H]IP_2 and [^{3}H]IP_3 formation was observed upon addition of PAF, with the peak response occuring between 30 and 60 sec (Fig. 1; see also Fig. 3). The PAF-induced production of [^{3}H]IP_1 increased slowly and then reached a plateau by 20–30 min after addition of PAF (Fig. 1). As shown in Fig. 2, the PAF-induced production of IP_3 and IP_1 was dependent on the concentration of the agonist (similar data for

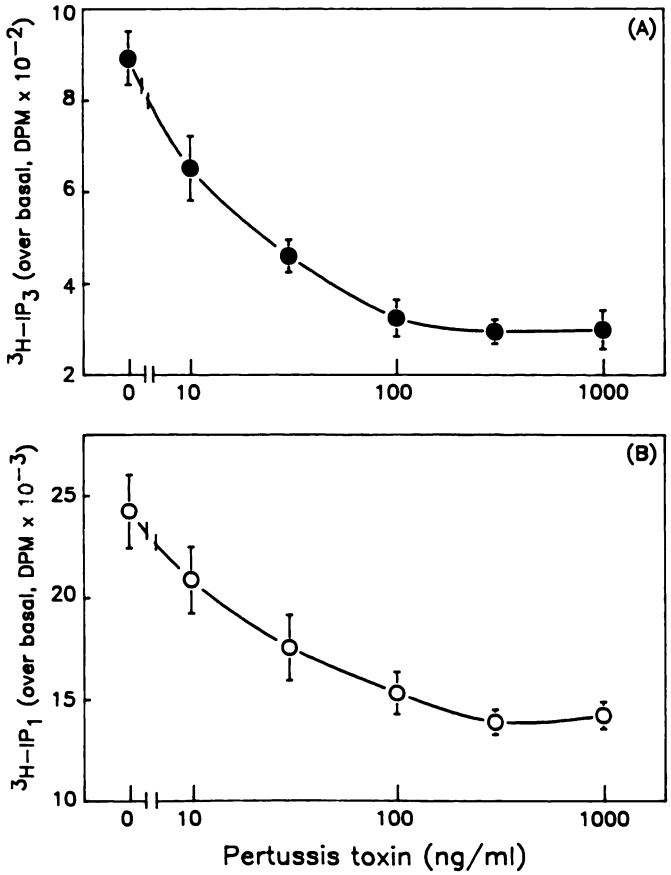

Fig. 7. Effects of PTX on PAF-induced production of [^{3}H]IP_3 (A) and [^{3}H]IP_1 in NCB-20 cells. Experimental conditions are as described in the legend (B) to Fig. 1, except that *myo*-[^{3}H]inositol-labeled NCB-20 cells were treated with vehicle or different concentrations of PTX, as indicated, for 16–18 hr before use. Cells were stimulated with 50 nM PAF or vehicle (basal) for 1 min (IP_3) or 30 min (IP_1). The inositol phosphates were separated and quantitated by open column chromatography, as described in Materials and Methods. Basal values of [^{3}H]inositol phosphates were not significantly affected by PTX. Each *point* is the mean of four or five experiments done in triplicate.

TABLE 3

Effect of PTX on PAF-induced elevation of $[Ca^{2+}]_i$ in NCB-20 cells

NCB-20 cells were pretreated with or without PTX for 16–18 hr. The cells were harvested, washed with KRH buffer, and then loaded with fura-2, as described in Materials and Methods. Cells were suspended in Ca^{2+}-free KRH buffer with 1 mM EGTA and were stimulated with 50 nM PAF, and $[Ca^{2+}]_i$ was quantitated immediately.

Treatment	$\Delta[Ca^{2+}]_i$	*n*
	nM	
PAF	94.3 ± 13.5	5
PAF + PTX (30 ng/ml)	54.6 ± 4.7[a]	6
PAF + PTX (300 ng/ml)	34.9 ± 7.0[b]	5

[a] $p < 0.05$, compared with PAF alone.
[b] $p < 0.01$, compared with PAF alone.

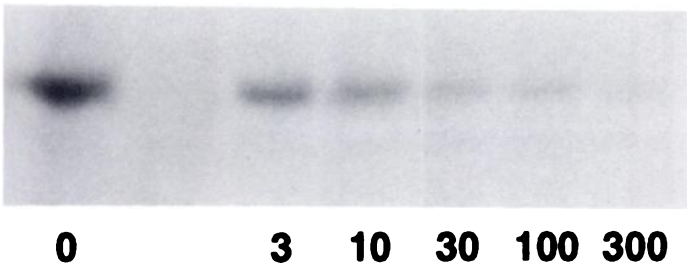

Fig. 8. [^{32}P]ADP-ribosylation by PTX of membranes prepared from NCB-20 cells preincubated with various concentrations of PTX, as indicated, for 16–18 hr at 37°. Membranes were then prepared from the cells and subsequently incubated with 5 μM [^{32}P]NAD in the presence (*lanes 1* and *3–7*) or absence (*lane 2*) of preactivated PTX at 5 μg/ml, as described in Materials and Methods. The membranes were then dissolved in SDS sample buffer. Electrophoresis was carried out on a 12-cm, 10% polyacrylamide gel. The gel was dried and exposed to Kodak XAR-5 film, in the presence of intensifying screens, overnight.

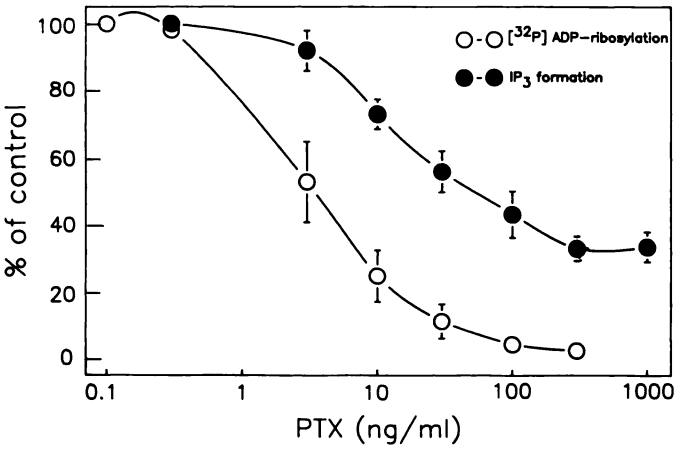

Fig. 9. Inhibiton of PAF-stimulated IP_3 formation and [^{32}P]ADP-ribosylation of 38-kDa membrane protein by pretreatment of NCB-20 cells with various concentrations of PTX. Experimental conditions were as described in the legends to Figs. 7 and 8. The [^{32}P]ADP-ribosylation autoradiograms were analyzed using the Hewlett-Packard DeskScan Image Analyzer, and the data were quantitated using Fotodyne's College Analysis Sofware. The data are the mean ± standard error obtained from four (ADP-ribosylation) or five (IP_3 formation) experiments.

IP_2 are not shown). Concentrations of PAF required for half-maximal stimulation (i.e., EC_{50}) of IP_3 and IP_1 production were 1.96 ± 0.62 nM and 1.12 ± 0.50 nM (n = 4), respectively, and the saturating concentration was approximately 50–100 nM (Fig. 2). PAF (50 nM) increased IP_3 and IP_1 production by 254 ± 34% and 178 ± 25% (n = 4) over basal after 1-min and 30-min stimulation, respectively.

Using anion exchange HPLC, the species of IP_3 induced by PAF were analyzed. As shown in Fig. 3, the production of 1,4,5-IP_3 was clearly apparent at 10 sec and reached maximum at 30–60 sec after addition of PAF. However, the biologically inactive isomer 1,3,4-IP_3 started to appear at 30 sec and was maximally increased at 5 min after stimulation with PAF.

Preincubation of NCB-20 cells with the PAF antagonist BN 50739 inhibited 50 nM PAF-induced production of IP_3 in a concentration-dependent manner (Table 1). The IC_{50} value of BN 50739 for inhibition of 50 nM PAF-induced IP_3 production was 6.48 ± 0.52 nM (n = 4). PAF-induced production of IP_1 was also inhibited by BN 50739. In the presence of 3 and 10 nM BN 50739, the formation of IP_1 was reduced by 25.1 ± 4.1%

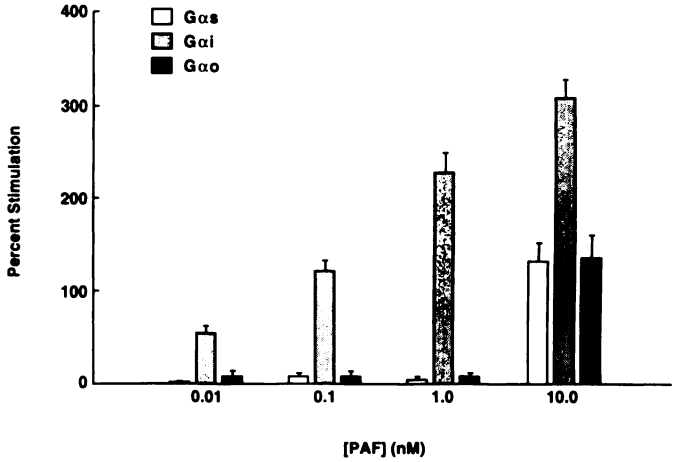

Fig. 10. Effect of PAF on activation of G_α proteins in NCB-20 cells. Aliquots of membrane preparations from NCB-20 cells were incubated for 5 min at 30° with 2 nM [^{35}S]GTPγS. Increasing concentrations of PAF were added, and incubation was continued for an additional 5 min. Membranes were solubilized, $G_{\alpha s}$, $G_{\alpha(1,2)}$, and $G_{\alpha o}$ proteins were immunoprecipitated, and radioactivity was determined. *Bars*, mean ± standard error of 4–10 determinations, as percentage of stimulation, for each G_α protein.

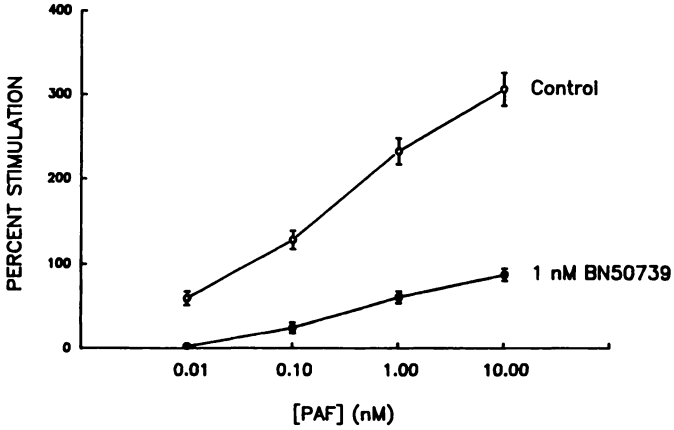

Fig. 11. Effect of PAF antagonist BN50739 on PAF-induced [^{35}S]GTPγS binding to membrane $G_{\alpha(1,2)}$ protein of NCB-20 cells. Aliquots of membrane preparation obtained from washed NCB-20 cells were incubated with or without 1 nM BN50739 for 5 min. The incubation was continued for an additional 5 min after the addition of 2 nM [^{35}S]GTPγS. PAF, in concentrations of 0.01–10.0 nM, was added, and the incubation was terminated after 5 min at 30°. Binding of [^{35}S]GTPγS was assessed in the precipitate after the addition of antibody to $G_{\alpha(1,2)}$, as described in Materials and Methods. Each *point* is the mean ± standard error of at least four individual determinations.

and 59.5 ± 7.2% (n = 3), respectively. BN 50739 had no effect on the basal levels of IP_3 and IP_1.

Effects of phorbol ester on PAF-induced PI turnover and elevation of $[Ca^{2+}]_i$ in NCB-20 cells. In NCB-20 cells the maximal accumulation of IP_3 (at 1 min) and IP_1 (at 30 min) induced by 50 nM PAF, over the basal level, was 962 ± 39 dpm and 16,315 ± 1,239 dpm (n = 3), respectively. Pretreatment of NCB-20 cells with the biologically active PDBu for 10 min at 37° reduced the PAF-induced formation of IP_3 and IP_1, in a dose-dependent manner (Fig. 4). The maximal inhibition of IP_3 and IP_1 formation was 87 ± 5% and 74 ± 4% (n = 3), respectively, in the presence of 1 μM PDBu. The IC_{50} values of PDBu for inhibition of PAF-induced formation of IP_3 and IP_1 were 79.3 nM and 38.2 nM, respectively. As shown in Fig. 4, the basal

TABLE 4

Effects of PTX on PAF-induced [^{35}S]GTP$_\gamma$S binding to membrane G proteins

Aliquots of membrane preparations from NCB-20 cells were preincubated for 2 hr at 37° with activated PTX (25 μg/mg of tissue). Tubes were incubated for 5 min at 30° with 2 nM [^{35}S]GTP$_\gamma$S before addition of PAF, and incubation was continued for an additional 5 min. Membranes were solubilized, $G_{\alpha s}$, $G_{\alpha i(1,2)}$, and $G_{\alpha o}$ proteins were immunoprecipitated, and radioactivity was determined.

	Stimulation	
	1 nM PAF (n = 10)	10 nM PAF (n = 10)
	%	
$G_{\alpha s}$	3.5 ± 2.8	110.3 ± 25.8
$G_{\alpha i(1,2)}$	230.8 ± 21.2	296.7 ± 20.7
$G_{\alpha o}$	7.0 ± 5.9	112.2 ± 29.3
	Stimulation	
	PTX + 1 nM PAF (n = 4)	PTX + 10 nM PAF (n = 4)
	%	
$G_{\alpha s}$	0.0 ± 0.0	88.8 ± 3.2
$G_{\alpha i(1,2)}$	38.0 ± 10.2[a]	70.3 ± 16.4[a]
$G_{\alpha o}$	0.0 ± 0.0	30.5 ± 4.6[b]

[a] $p < 0.01$, compared with the respective PAF-induced response.
[b] $p < 0.05$.

accumulation of IP_3 and IP_1 was not significantly affected by PDBu. The biologically inactive 4α-PDD did not affect PAF-induced IP_3 and IP_1 production or basal levels.

In the presence of 300 nM PDBu, the dose-response curve of PAF for inducing $[Ca^{2+}]_i$ elevation in NCB-20 cells was shifted rightward, and the maximal response of PAF was greatly reduced (Fig. 5A). As shown in Fig. 5B, the inhibitory effect of PDBu on 50 nM PAF-induced $[Ca^{2+}]_i$ elevation was dose dependent. The maximal inhibition was 81 ± 4%, with an IC_{50} value of 94 ± 8 nM (n = 4). Fig. 5B, *inset*, shows the time course of PDBu inhibition of 50 nM PAF-induced $[Ca^{2+}]_i$ elevation in NCB-20 cells. After a 5-min pretreatment of cells with 300 nM PDBu, the inhibitory effect on PAF-induced $[Ca^{2+}]_i$ elevation reached a plateau. The biologically inactive 4α-PDD (1 μM) had no effect on the PAF-induced increase in $[Ca^{2+}]_i$ in NCB-20 cells (data not shown). The inhibitory effects of PDBu on the PAF-induced $[Ca^{2+}]_i$ rise and PI turnover in NCB-20 cells could be partially reversed by the PKC inhibitor H-7. The inhibition by PDBu (100 nM) of the PAF-induced $[Ca^{2+}]_i$ elevation was reduced from 60.7 ± 3.9% to 33.9 ± 6.4% (n = 6, $p < 0.01$) after pretreatment of the cells with H-7 (100 μM) for 5 min before addition of PDBu (Fig. 6). Likewise, the inhibition by PDBu (100 nM) of PAF-induced IP_3 formation decreased from 53.3% to 36.1% after pretreatment of NCB-20 cells with 100 μM H-7 (Table 2). H-7 in the absence of PDBu had no effect on PAF-induced $[Ca^{2+}]_i$ elevation or IP_3 formation.

Effect of PTX on PAF-induced PI turnover in NCB-20 cells. Pretreatment of NCB-20 cells with PTX overnight (16–18 hr) significantly reduced PAF-induced production of IP_3 and IP_1, in a dose-dependent manner (Fig. 7). The maximal inhibition of 50 nM PAF-induced IP_3 and IP_1 formation was 66.9 ± 3.5% and 45.8 ± 4.3%, respectively, with a PTX concentration of 300 ng/ml (n = 4). Increasing the PTX concentration further did not increase the inhibitory effect on PAF-induced PI turnover (Fig. 7). PTX inhibited PAF-induced IP_2 production to a similar degree as IP_3 production (data not shown). The PAF-induced increase in $[Ca^{2+}]_i$ in NCB-20 cells was only moderately reduced (16.6 ± 6.5%, $p > 0.05$, n = 4) by PTX (300 ng/ml) when the cells were suspended in KRH buffer; however, the inhibitory effect of PTX on the PAF-induced intracellular Ca^{2+} release increased substantially when the cells were suspended in Ca^{2+}-free KRH buffer (Table 3). PTX had no effect on basal levels of inositol phosphates and $[Ca^{2+}]_i$ in NCB-20 cells.

PTX-induced ADP-ribosylation of a 38-kDa membrane protein in NCB-20 cells. Exposure of membranes prepared from NCB-20 cells to [^{32}P]NAD and preactivated PTX resulted mainly in a single band of radioactivity, with an apparent mass of approximately 38 kDa (Fig. 8, *lane 1*), indicating the incorporation of [^{32}P]NAD into the protein due to PTX-induced ADP-ribosylation of the substrate. Pretreatment of the cells with various concentrations of PTX inhibited, in a dose-dependent manner, the incorporation of [^{32}P]ADP-ribose into the substrate protein during the subsequent membrane-labeling experiment (Figs. 8 and 9). The maximal inhibiton was observed when the concentration of PTX reached 100–300 ng/ml, and nearly all the ADP-ribosylatable protein was inhibited. The EC_{50} for PTX inhibition of ADP-ribosylation was 3.39 ± 0.37 ng/ml (n = 4). Fig. 9 compares the effects of pretreatment of NCB-20 cells with PTX on PAF-induced IP_3 formation and [^{32}P]ADP-ribosylation.

Effect of PAF on the activation of G_α proteins in NCB-20 cells. Incubation of NCB-20 cell membranes with increasing concentrations of PAF (0.01–10 nM) elicited a concentration-related stimulation of [^{35}S]GTPγS binding to $G_{\alpha i(1,2)}$ protein; increased binding to $G_{\alpha s}$ and $G_{\alpha o}$ was observed only at the highest concentration of PAF tested (10 nM) (Fig. 10). PAF-induced [^{35}S]GTPγS binding to $G_{\alpha i(1,2)}$ protein was markedly inhibited by the PAF antagonist BN 50739 (Fig. 11). In addition, PAF-evoked activation of $G_{\alpha i(1,2)}$ was significantly reduced by preincubation with PTX (Table 4) but not cholera toxin (data not shown).

Discussion

In the present study, we have demonstrated that in NCB-20 cells PAF induces a rapid formation of inositol phosphates, including the calcium-mobilizing second messenger 1,4,5-IP_3. The EC_{50} values for PAF-induced formation of IP_3 and IP_1 were 1.96 nM and 1.12 nM, respectively, close to the EC_{50} value of 2.6 nM for PAF-induced $[Ca^{2+}]_i$ mobilization (Fig. 5A). The peak increase in IP_3 production appeared at 1 min (Fig. 1), which was delayed relative to the peak increase in $[Ca^{2+}]_i$ (Fig. 6). The reason for this apparent discrepancy might be due to the fact that IP_3 separated by the open column of anion exchange resin (shown in Fig. 1) represents multiple isomers, including 1,4,5-IP_3 and 1,3,4-IP_3, whereas only 1,4,5-IP_3 has been found to be able to stimulate Ca^{2+} release from intracellular stores. It has been found in animal tissues, including brain, that 1,4,5-IP_3 can be metabolized to form 1,3,4,5-IP_4, which is further metabolized to 1,3,4-IP_3 (23). Therefore, the appearance of 1,3,4-IP_3 would be delayed relative to 1,4,5-IP_3. The results from HPLC shown in Fig. 3 solved this apparent paradox. The 1,4,5-IP_3 peak was apparent as early as 10 sec and reached maximal levels by 30–60 sec after addition of PAF. However, 1,3,4-IP_3 started to appear at 30 sec after stimulation by PAF and continued to increase up to 5 min.

PAF-induced IP_3 formation was inhibited by the specific PAF antagonist BN 50739 (17) in a concentration-dependent manner, with an IC_{50} value of 6.5 nM. This was in agreement

with the IC_{50} value of 11.9 nM for the inhibition of PAF-induced $[Ca^{2+}]_i$ mobilization reported in our previous study (16). These data indicate that PAF interacts with specific receptors on NCB-20 cells to regulate inositol phosphate production as well as $[Ca^{2+}]_i$ mobilization.

In order to obtain further information on PAF-induced activation of PLC, the effects of phorbol esters were studied. PAF-induced $[Ca^{2+}]_i$ elevation and formation of IP_3 and IP_1 were inhibited by PDBu in a dose-dependent manner. In contrast, neither PI turnover nor $[Ca^{2+}]_i$ mobilization induced by PAF was affected by the biologically inactive 4α-PDD. These data are in agreement with previous reports that PAF-induced Ca^{2+} mobilization in endothelial cells and vascular smooth muscle cells (24) is blocked by pretreatment with PKC activators. The IC_{50} value of PDBu for inhibiting PAF-induced IP_3 formation (79.3 nM) is close to the IC_{50} value of PDBu for reducing PAF-induced $[Ca^{2+}]_i$ elevation (94 nM), suggesting that the effect of PDBu on $[Ca^{2+}]_i$ may be related to inhibition of PI turnover. The inhibitory effect of PDBu on both the $[Ca^{2+}]_i$ rise and PI turnover induced by PAF in NCB-20 cells was partially reversed by pretreatment with the PKC inhibitor H-7, supporting the hypothesis that PDBu inhibition is mediated through PKC activation. However, increasing the concentration of H-7 did not completely prevent the effects of PDBu. This may be due to a non-PKC-activatable component of PAF receptor signaling or additional activities of PDBu and H-7. For example, H-7 has been shown to act at the ATP binding site and inhibit other protein kinases (25), whereas phorbol esters can cause membrane perturbation at high concentrations (26). We tested another more potent and commonly used PKC inhibitor, staurosporine. However, NCB-20 cells were sensitive to the toxic effect of this agent. In a previous study (16), we reported that PAF-induced $[Ca^{2+}]_i$ mobilization in NCB-20 cells involves both influx of extracellular Ca^{2+} (64%) and release of intracellular Ca^{2+} (36%). The present data appear to indicate that PDBu inhibited PAF-induced $[Ca^{2+}]_i$ elevation not only via inhibiton of PAF-induced IP_3 formation but also by affecting PAF receptor-operated calcium channels. It has been reported that the phorbol ester inhibits binding of PAF to neutrophils (26) and reduces the affinity of insulin receptors in lymphocytes (27) and endothelin receptors in neurohybrid NG108-15 cells (28). However, it has also been reported that the phorbol ester increases insulin binding in glial cells (29) and angiotensin II binding in neurons (30). Whether the phorbol ester induces phosphorylation of PAF receptors or affects G protein-effector coupling requires further elucidation, but from the present data it is likely that PDBu has an effect at the PAF receptor. In this regard, our results suggest that PAF-induced PKC activation may serve as negative feedback to protect against cellular overstimulation. On the other hand, PDBu did not affect the basal levels of inositol phosphates and $[Ca^{2+}]_i$, suggesting that the activation of PKC does not affect the basal activity of PLC and basal Ca^{2+} homeostasis.

Receptor-mediated activation of PLC involves a G protein, which serves as a coupling unit between the receptor and the effector PLC and is often referred to as "G_p" (31). Studies with human neutrophils point to the existence of PTX-sensitive G_p coupled to PAF receptors (5). Conversely, treatment of human platelet membranes with PTX had no effect on GTPase activity stimulated by PAF (32). Similar results were also recently reported in U937 cells, a human monocytic leukemic cell line, in which neither $[Ca^{2+}]_i$ mobilization nor PI turnover induced by PAF was sensitive to PTX (33). These data suggest that not only are the G proteins coupled to various receptors different but the G proteins coupled to the same receptor in diverse cell types also may be different. The present results directly demonstrate that at least three α subunits of G proteins exist in NCB-20 cells and PAF receptors couple selectively to $G_{\alpha i(1,2)}$, compared with $G_{\alpha s}$ or $G_{\alpha o}$, especially at a low concentration of PAF (1 nM) (Fig. 10; Table 4). The results also suggest that the PTX-sensitive response to PAF in NCB-20 cells is likely to be mediated mainly through the activation of membrane $G_{\alpha i(1,2)}$ protein. PAF-induced [^{35}S]GTPγS binding to $G_{\alpha i(1,2)}$ and $G_{\alpha o}$ was significantly reduced by pretreatment with PTX. This is in agreement with the finding that pretreatment of NCB-20 cells with PTX resulted in significant reduction of PAF-induced increases in IP_3 and IP_1 formation and intracellular Ca^{2+} release. It is known that the molecular basis of PTX action is a toxin-catalyzed ADP-ribosylation of G protein, using NAD as ADP-ribosyl donor (34), resulting in uncoupling of receptor and effector. To further determine whether a PTX-promoted modification of G protein (i.e., ADP-ribosylation) was related to the ability of the toxin to inhibit PAF-stimulated PI metabolism and intracellular Ca^{2+} release, membranes were prepared from NCB-20 cells that had been exposed to various concentrations of PTX. These membranes were subsequently radiolabeled in the presence of [^{32}P]NAD and preactivated toxin. The result of PTX labeling shows that pretreatment of the cells with PTX resulted in a dose-dependent inhibition of [^{32}P] ADP-ribosylation of a 38-kDa membrane protein, indicating that the pretreatment had inactivated the G protein (Figs. 8 and 9). Moreover, at 100–300 ng/ml PTX, the entire pool of PTX-sensitive G proteins in NCB-20 cells was ADP-ribosylated by the pretreatment, which correlated well with the concentration of PTX producing maximal inhibition of PAF-induced PI metabolism (Figs. 7 and 9) and intracellular Ca^{2+} release (Table 3). However, the maximal inhibition by PTX of PAF-induced IP_3 formation was 67%, and no greater inhibition was achieved by increasing the concentration of PTX further (Fig. 9), suggesting that a PTX-insensitive pathway is also involved in PAF-stimulated PI turnover. This is in agreement with the results in Table 4 showing that PAF-induced [^{35}S] GTPγS binding to $G_{\alpha s}$ was not affected by pretreatment with PTX. Our data may also be in agreement with a recent report by Smrcka *et al.* (35), who isolated a new PTX-insensitive G protein (G_q), which is linked to PLC in bovine brain. Moreover, pretreatment of the cells with PTX had only modest effects on PAF-induced Ca^{2+} influx, indicating that PAF receptor-operated Ca^{2+} channels appear to be minimally affected by PTX. It is suggested from these results that both PTX-sensitive and -insensitive G proteins are involved in PAF receptor-mediated signal transduction in NCB-20 cells.

In conclusion, the present study demonstrates that PAF stimulates PI metabolism in NCB-20 cells through receptor activation and that the PAF-induced production of IP_3 is correlated with PAF-induced $[Ca^{2+}]_i$ mobilization. Phorbol ester inhibited the PAF-induced increase in PI turnover and rise in $[Ca^{2+}]_i$, which could be partially prevented by the PKC inhibitor H-7, indicating the involvement of PKC in the regulation of the PAF-induced signal transduction. PAF receptors appear to be selectively coupled to $G_{\alpha i}$ proteins, and PAF signal transduction is mediated by both PTX-sensitive and -insensi-

tive pathways. These results may contribute to the further understanding of the mechanism of PAF action on neuronal cells.

References

1. Snyder, F. Platelet-activating factor and related acetylated lipids as potent biologically active cellular mediators. *Am. J. Physiol.* **259**:C697–C708 (1990).
2. Braquet, P., L. Touqui, T. Shen, and B. Vargafting. Perspectives in platelet-activating factor research. *Pharmacol. Rev.* **39**:97–145 (1987).
3. Honda, Z., M. Nakamura, I. Miki, M. Minami, T. Watanabe, Y. Seyama, H. Okado, H. Toh, K. Ito, T. Miyamoto, and T. Shimizu. Cloning by functional expression of platelet-activating factor receptor from guinea-pig lung. *Nature (Lond.)* **349**:342–346 (1991).
4. Hwang, S. B. Specific receptors of platelet-activating factor, receptor heterogeneity, and signal transduction mechanism. *J. Lipid Mediators* **2**:122–158 (1990).
5. Hwang, S. B. Identification of a second putative receptor of platelet-activating factor from human polymorphonuclear leukocytes. *J. Biol. Chem.* **263**:3225–3233 (1988).
6. Tokumura, A., K. Kamiyasu, and H. Tsukatani. Evidence for existence of various homologues and analogues of platelet-activating factor in a lipid extract of bovine brain. *Biochem. Biophys. Res. Commun.* **145**:415–425 (1987).
7. Kumar, R., S. A. K. Harvey, M. Kester, D. J. Hanahan, and M. S. Olsin. Production and effects of platelet-activating factor in the rat brain. *Biochim. Biophys. Acta* **963**:375–383 (1988).
8. Lindsberg, P. J., T. L. Yue, K. U. Frerichs, J. M. Hallenbeck, and G. Feuerstein. Evidence of platelet-activating factor (PAF) as a noval mediator in experimental stroke in rabbits. *Stroke* **21**:1452–1457 (1990).
9. Yue, T. L., P. G. Lysko, and G. Feuerstein. Production of platelet-activating factor from rat cerebellar granule cells in culture. *J. Neurochem.* **54**:1809–1811 (1990).
10. Sogos, V., F. Bussolino, E. Pilia, S. Torelli, and F. Gremo. Acetylcholine-induced production of platelet-activating factor by human fetal brain cells in culture. *J. Neurosci. Res.* **27**:706–711 (1990).
11. Marcheselli, V. L., M. J. Rossowska, M. T. Domingo, P. Braquet, and N. G. Bazan. Distinct platelet-activating factor binding sites in synaptic endings and in intracellular membranes of rat cerebral cortex. *J. Biol. Chem.* **265**:9140–9145 (1990).
12. Domingo, M. T., B. Spinnewyn, P. E. Chabrier, and P. Braquet. Presence of specific binding sites for platelet-activating factor (PAF) in brain. *Biochem. Biophys. Res. Commun.* **151**:730–736 (1988).
13. Feuerstein, G., T. L. Yue, and P. G. Lysko. Platelet-activating factor: a putative mediator in central nervous system injury? *Stroke* **21** (Suppl. III):90–94 (1990).
14. Kochanek, P. M., E. M. Nemoto, J. A. Melick, R. W. Evans, and D. F. Burker. Cerebrovascular and cerebrometabolic effects of intracarotid infused platelet-activating factor in rats. *J. Cereb. Blood Flow Metab.* **8**:546–551 (1988).
15. Lindsberg, P. J., T. P. Jacobs, I. A. Paakkari, J. M. Hallenbeck, and G. Feuerstein. Effect of systemic platelet-activating factor (PAF) on the rabbit spinal cord microcirculation. *J. Lipid Mediators* **2**:41–58 (1990).
16. Yue, T. L., M. M. Gleason, J. Hallebeck, and G. Feuerstein. Characterization of platelet-activating factor-induced elevation of cytosolic free calcium level in neurohybrid NCB-20 cells. *Neuroscience* **41**:177–185 (1991).
17. Yue, T. L., R. Rabinovici, M. Farhat, and G. Feuerstein. Pharmacologic profile of BN 50739, a new PAF antagonist *in vitro* and *in vivo*. *Prostaglandins* **39**:469–480 (1990).
18. Hawkins, P. T., L. Stephens, and C. P. Downes. Rapid formation of inositol 1,3,4,5-tetrakisphosphate and inositol 1,3,4-trisphosphate in rat parotid glands may both result indirectly from receptor-stimulated release of inositol 1,4,5-trisphosphate from phosphatidylinositol 4,5-bisphosphate. *Biochem. J.* **238**:507–516 (1986).
19. Yue, T. L., M. M. Gleason, P. G. Lysko, and G. Feuerstein. Effect of endothelins on cytosolic free calcium concentration in neuroblastoma NG108-15 and NCB-20 cells. *Neuropeptides* **17**:7–12 (1990).
20. Lowry, O. H., N. J. Rosebrough, A. L. Farr, and R. J. Randall. Protein measurement with the Folin phenol reagent. *J. Biol. Chem.* **193**:265–275 (1951).
21. Romano, C., R. A. Nichols, P. Greengard, and L. A. Greene. Synapsin 1 in PC12 cells. 1. Characterization of the phosphoprotein and the effect of chronic NGF treatment. *J. Neurosci.* **7**:1294–1299 (1987).
22. Clark, M. A., T. M. Conway, F. Bennett, S. T. Crooke, and J. M. Stadel. Islet-activating protein inhibits leukotriene D_4- and leukotriene C_4- but not bradykinin- or calcium ionophore-induced prostacyclin synthesis in bovine endothelial cells. *Proc. Natl. Acad. Sci. USA* **83**:7320–7324 (1986).
23. Irvine, R. F., A. J. Letcher, J. P. Heslop, and M. J. Berridge. The inositol tris/tetrakisphosphate pathway: demonstration of Ins(1,4,5)P_3 3-kinase activity in animal tissues. *Nature (Lond.)* **320**:631–634 (1986).
24. Schwertschlag, U. S., and A. R. Whorton. Platelet-activating factor-induced homologous and heterologous desensitization in cultured vascular smooth cells. *J. Biol. Chem.* **263**:13791–13796 (1988).
25. Ruegg, U. T., and G. M. Burgess. Staurosporine, K-252 and UCN-01: potent but nonspecific inhibitors of protein kinases. *Trends Pharmacol. Sci.* **10**:218–220 (1989).
26. Yamazaki, M., J. Gomez-Cambronero, M. Durstin, T. F. P. Molski, E. Becker, and R. I. Sha'afi. Phorbol 12-myristate 13-acetate inhibits binding of leukotriene B_4 and platelet-activating factor and the responses they induce in neutrophils: site of action. *Proc. Natl. Acad. Sci. USA* **86**:5791–5794 (1989).
27. Grunberger, G., and P. Gorden. Affinity alteration of insulin receptor induced by a phorbol ester. *Am. J. Physiol.* **243**:E319–E324 (1982).
28. Yue, T. L., P. Nambi, H. L. Wu, and G. Feuerstein. Endothelin receptor and cellular signal transduction in neurohybrid NG108-15 cells. *Neuroscience*, **44**:215–222 (1991).
29. Mudd, L. M., and M. K. Raizada. Phorbol esters increase insulin binding in astrocytic glial but not neuronal cells in primary culture from the brain. *Brain Res.* **521**:192–196 (1990).
30. Sumners, C., S. M. Rueth, L. M. Myers, C. J. Kalberg, F. T. Crews, and M. K. Raizada. Phorbol ester-induced up-regulation of angiotensin II receptors in neuronal cultures is potentiated by a calcium ionophore. *J. Neurochem.* **51**:1–8 (1988).
31. Birnbaumer, L., J. Abramowitz, and A. M. Brown. Receptor-effector coupling by G proteins. *Biochem. Biophys. Acta* **1031**:163–224 (1990).
32. Houslay, M. D., D. Bojanic, D. Gawler, S. O'Hagan, and A. Wilson. Thrombin, unlike vasopressin, appears to stimulate two distinct guanine nucleotide regulatory proteins in human platelets. *Biochem. J.* **238**:109–113 (1986).
33. Barzaghi, G., H. M. Sarau, and S. Mong. Platelet-activating factor-induced phosphoinositide metabolism in differentiated U-937 cells in culture. *J. Pharmacol. Exp. Ther.* **248**:559–566 (1989).
34. Hayaishi, O., and K. Ueda. Poly- and mono(ADP-ribosyl)ation reactions: their significance in molecular biology, in *ADP-Ribosylation Reactions* (O. Hayaishi and K. Ueda, eds.). Academic Press, New York, 3–16 (1982).
35. Smrcka, A. V., J. R. Hepler, K. O. Brown, and P. C. Sterweis. Regulation of polyphosphoinositide-specific phospholipase C activity by purified G_q. *Science (Washington D. C.)* **251**:804–807 (1991).

Send reprint requests to: Tian-Li Yue, Ph.D., Department of Pharmacology, SmithKline Beecham Pharmaceuticals, L-510, P.O. Box 1539, King of Prussia, PA 19406-0939.